J4.2 INTERMITTENT BURSTING OF TURBULENCE IN A STABLE BOUNDARY LAYER WITH LOW-LEVEL JET

Yuji Ohya*, Reina Nakamura and Takanori Uchida***

***Research Institute for Applied Mechanics, Kyushu University, Japan**

****Dept. of Meteorological Environment, Forestry and Forest Products Research Institute, Japan**

List of Symbols

g	acceleration due to gravity
Re_δ	Reynolds number based on δ ($= U_\infty \delta / \nu$)
Ri_δ	bulk Richardson number($= g \delta \Delta \Theta / \Theta_o U_\infty^2$)
Ri	local gradient Richardson number ($= (g/\Theta) \cdot (\partial \Theta / \partial z) / (\partial U / \partial z)^2$))
U_∞	freestream velocity
U_{max}	maximum value of mean streamwise velocity of LLJ
U, W	mean velocity components in x and z directions
u, w	fluctuating velocity components in x and z directions
uw	vertical turbulent momentum flux
$u\theta$, $w\theta$	horizontal and vertical turbulent heat fluxes
δ	boundary layer thickness where U-velocity shows a maximum value
μ, υ	coefficients of dynamic and kinematic viscosity
Θ	mean temperature
Θ_∞	temperature of ambient air
Θ_s	temperature of cooled floor
$\triangle\Theta$	temperature difference ($= \Theta_\infty - \Theta_s$)
Θ_o	average absolute temperature in boundary layer
θ	fluctuating temperature
σ_u, σ_w, σ_θ	standard deviation of u, w and θ fluctuations

1. INTRODUCTION

The atmospheric boundary layer under stable stratification (Stable Boundary Layer or SBL hereafter) is difficult to describe and model. With increasing stability, turbulence in SBLs becomes intermittent and patchy, allowing the upper portion of the boundary layer to decouple from surface forcings (Stull, 1988; Mahrt, 1999). With the use of a wind tunnel, we have been investigating the nature of turbulent flows in SBLs over a wide range of stability (Ohya, et al., 1997; Ohya, 2001; Ohya and Uchida, 2003). In our past wind tunnel experiments for SBLs, vertical profiles of the mean wind velocity resembled those in typical turbulent boundary layers. However, SBLs from field observations are often accompanied with a low-level jet (LLJ). Namely, stable stratification and a strong wind shear coexist near the ground.

In the present study, we designed a wind tunnel specifically for simulating SBLs with a LLJ. To produce thermally stratified flows, the tunnel is equipped with two independent temperature systems, which consist of an airflow heating unit and a floor temperature-controlling unit. To simulate a LLJ, a non-uniform vertical screen was located in the upstream section of the wind tunnel. Under certain conditions, we observed intermittent turbulence bursting and report the result here.

While intermittent turbulence is frequently observed in the atmospheric stable boundary layers, the origin of the intermittency is not well understood (Mahrt, 1999). Thus, no appropriate parameterization is yet available for simulating intermittent turbulence in numerical atmospheric models. Some field studies in the past, however, indicated intermittent turbulence appears as a result of the local Richardson number being lowered due to the passage of gravity currents and gravity waves and the emergence of Kelvin-

**Corresponding author address* : Yuji Ohya, Research Institute for Applied Mechanics, Kyushu University, 6-1 Kasuga-koen, Kasuga 816-8580, Japan ; e-mail : ohya@riam.kyushu-u.ac.jp

Helmholtz instability. Thus, reduction in the Richardson number appears to be a key factor for generation of intermittent turbulence.

In the present study, intermittent turbulence produced in a stably stratified wind tunnel is examined. The cause and features of intermittent turbulence are investigated with an emphasis of the interaction of intermittent turbulence with the local Richardson number.

2. THERMALLY STRATIFIED WIND TUNNEL AND EXPERIMENTAL METHOD

2.1 *Wind Tunnel*

Experiments were performed in a thermally stratified wind tunnel at Kyushu University (Ohya et al., 1996). The wind tunnel is of a suction type and has a rectangular test section of 1.5m wide, 1.2m high and 13.5m long. Designed to produce thermally stratified flows, the wind tunnel is equipped with two independent temperature systems: an air-flow heating unit (AHU) and a floor temperature controlling unit (FTCU). The AHU, which consists of 40 horizontal plates separated by 3cm, is positioned upstream of the test section. The air-flow passing through each story is individually heated up to 150℃ by two electric heater rods at wind speed of 1 m s^{-1} and can be set to a desired temperature by a PID feedback system. To provide a uniform smooth flow with low turbulence intensity, the downstream side of this unit is equipped with a honeycomb in each story and two screens. The FTCU consists of a refrigerator, water tanks with electric heaters and 10 floor panels. Each floor panel is 1.5m wide and 1.0m long. Heated or cooled water flows through the panel to achieve a uniform temperature distribution on the panel surface. The test section is covered by thermal insulation on both walls and the ceiling and is made of a double sidewall arrangement to avoid a secondary flow in the test section. With the use of the AHU and FTCU, a wide range of thermal stratification can be achieved with freestream velocity in the range of 0.2-2.0 m s^{-1}.

2.2 *Experimental Method*

The experimental arrangement for the present SBL simulation with a LLJ is shown in Figure 1. The boundary layer is artificially tripped by a two-dimensional (2D) 5-cm tall fence at the entrance of the test section. The flow condition upstream of the 2D fence is smooth and uniform with turbulence intensity of less than 1.0%. The SBL flows, where the mean temperature increases with height, are generated by heating the wind-tunnel airflow to approximately 40℃ and by cooling the test-section floor to approximately 11℃. To simulate a LLJ, we set up a non-uniform vertical screen (the resistance screen) at 6m downstream from the 2D fence.

We ran two experiments: one with a weakly stable boundary layer (S1) and one with a highly stable boundary layer. Details of the flow are given in Table 1. The Reynolds number, Re_δ, based on the LLJ height, δ, ranges from (1.3–1.6)x10^4 and the bulk Richardson number, Ri_δ (=$(g/\Theta_o) \cdot (\Theta_\infty - \Theta_s)\,\delta / U_{max}^2$), ranges from 0.07 to 0.13. Here, U_{max} is the maximum air speed of the LLJ and Θ_∞ is the temperature at the height of U_{max}. The temperatures, Θ_s and Θ_o are the surface and reference temperatures, respectively.

Measurements of turbulent quantities in the vertical direction are made at 9m downstream from the 2D fence and at 3m downstream from the resistance screen (Figure 1). The velocity and temperature fluctuations are measured simultaneously using an X-type hot-wire and an I-type cold-wire. Calibration was carried out in a special calibration unit that can provide a controlled airflow at a specified wind speed and temperature (Ohya and Fukamachi, 1997). For data acquisition, three channels of amplified signals are first low-pass filtered at 200 Hz and digitized by an A/D converter (12 bit) at a sampling frequency of 500Hz. The data sampling period is approximately 100 - 150s for each height. Flow visualization of the simulated SBL flows is also carried out with a smoke-wire device deployed inside the test section.

3. RESULTS

3.1 Vertical Profiles of Turbulent Quantities

Figures 2 and 3 show vertical profiles of the mean temperature Θ and mean *U*-velocity. Stably stratified flows, in which the mean temperature increases with height in a polynomial manner, are successfully generated (Figure 2). The maximum wind speed, a LLJ, is evident near the surface for both cases S1 and S2, leading to a strong near-ground wind shear.

Figures 4-6 show vertical profiles of normalized fluctuation intensities (σ :standard deviation) of *u-*, *w*-velocity components and

temperature θ , respectively. The stable stratification suppresses velocity and temperature fluctuations. These fluctuations decrease with increasing stability (Ohya, 2001) and so do momentum and heat fluxes (Figures 7-9).

3.2 *Time Series of Velocity and Temperature Fluctuations*

Figure 10 shows time series of *w*-velocity fluctuations for both the S1 and S2 cases observed at *z*=20mm from the surface. The upper figure for case S1 (weakly stable) indicates large-amplitude and high-frequency turbulent motions, showing vigorous turbulent mixing in the lower part of the boundary layer, similar to the neutral flow case. On the other hand, as shown in the lower figure for case S2 (highly stable), intermittent turbulence bursting is frequently observed. Hereafter, we discuss case S2.

Our experimental set-up allowed simultaneous measurements of *u*, *w* and θ at a single height at a time. Therefore, a set of the three variables was captured in a different time period for each height (*z* = 5 - 60mm) (Figures 11 – 13). The time series of *w*-velocity fluctuations (Figure 11) indicates that turbulence bursting appears mainly in the range of *z*=20-40mm. In the range of *z*<20mm and *z*>40mm, turbulence bursting occurs less frequently and the amplitude of the bursting is rather small. The same phenomena are observed in the time series of *u*-velocity and temperature fluctuations (Figures 12 and 13). At *z* = 5-10mm, *u*-velocity and temperature decrease immediately before bursting while they increase immediately after bursting. On the other hand, at *z*=30-40mm, both *u*-velocity and temperature decrease during bursting events. These observations suggest that bursting, which dominantly appears at approximately *z*=20-30mm, brings fluid with relatively low velocity and temperature upward and brings fluid with relatively high velocity and temperature downward.

With cessation of turbulence bursting, fluctuations of wind velocity and temperature in the vertical range of *z*=0-30mm (z/δ=0-0.2) are very small and indicate a near non-turbulent state (Figures 11 – 13); therefore, in this vertical range, the turbulence intensities, σ of velocity and temperature in Figure 4-6 are very small, close to zero. Boundary layers with these types of vertical profiles of turbulence intensities are classified as highly stable boundary layers (Ohya, et al., 1997 and Ohya, 2001). Thus, case S2 is considered as a highly stable boundary layer with occasional turbulence bursting.

To investigate the nature of turbulence bursting in detail, we made additional measurements of *u*, *w* and θ simultaneously at two different heights for case S2. Figure 14 shows the simultaneous measurement of *w*-velocity fluctuations at *z*=10mm and 30mm. Comparing these two time series of *w*-velocity, we confirmed that the influence of turbulence bursting propagates downward from *z*=30mm to *z*=10mm. Thus, turbulence bursting originates in the lower part of the boundary layer, however, away from the surface.

3.3 *Flow Visualization of SBL with LLJ*

Flow visualizations of the simulated SBL with a LLJ were carried out with a smoke-wire device made of several horizontal nichrome wires. The device was set normal to the flow direction at *x*=8m, and smoke released from the wire visualized streaklines of the flow. Figure 15 shows the side view of an instantaneous SBL flow field with a LLJ at approximately *x*=9m for case S2. Both photos capture the moment of onset of turbulence bursting. A bursting event is confined to the vertical range between the surface and approximately *z*=60mm. The height of the origin of a bursting event is approximately *z*=20-25mm; that is, bursting does not originate at the surface, but aloft away from the surface. Turbulence bursting generated aloft spreads both upward and downward immediately downstream of the generated bursting. The height of the origin of bursting captured in Figure 15 corresponds to the height with most frequent bursting in Figures 11-13.

3.4 *Mechanism of Intermittent Turbulence Bursting*

Furthermore, we investigated the behavior of the local gradient Richardson number both during and in the absence of turbulence bursting for case S2. The gradient Ri number (Figure 16) is evaluated using u-velocity and temperature measured simultaneously at *z*=30 and 43mm (Δ *z*=13mm). To show the variations of the Ri number smoothly, a moving-average over 0.3s is adopted. Temporal variations of simultaneously measured *w*-velocity and the gradient Ri number (Figure 16) show high correlation. During a bursting event, the Ri number becomes smaller than the critical Ri number, Ri_{cr} =0.25 while the Ri number becomes larger than the Ri_{cr} number in the absence of a

bursting event.

For stably stratified flows, turbulent flow is suppressed by buoyancy. We speculate that wind shear increases locally in stable boundary layers because of a lack of mixing. Eventually, shear becomes large enough to trigger shear instability thus turbulence (i.e., the local Richardson number becomes lower than Ri_{cr}). The resulting turbulence mixes both heat and momentum, causing the shear to decrease and the Richardson number to increase. Eventually, the shear is too weak to support shear instability and turbulence, and they both cease. During the quiescent period, shear can again build to the point of shear instability thus turbulence. Such a scenario can occur repeatedly (Stull, 1988 ; Mahrt, 1999).

3.5 *Comparison with Intermittent Turbulence Observed in Atmospheric Stable Boundary Layers*

Similar intermittent turbulence bursting is observed in field measurements (Kondo et al., 1978, Sun et al. 2000, 2002, and Nakamura and Mahrt, 2005). Kondo et al. (1978) reported intermittent turbulence observed near the ground at *z*=4.4m; the time series of w-component velocity, temperature and vertical heat flux illustrate repeated occurrence of turbulent and non-turbulent flow states. The time series of the gradient Richardson number in the same period shows small and large values in the turbulent and non-turbulent periods, respectively. This observation is very similar to the result in Figure 16.

Sun et al. (2000 and 2002) reported intermittent turbulence associated with a density current passage in a highly stable boundary layer from CASES-99. Due to the passage of the density current, wind velocity increased near the ground. The resulting strong wind shear led to a decrease in the Ri number, generating turbulence bursting eventually. This event is evident in w-velocity and temperature fluctuations measured with an ultra-sonic anemometer and thermocouples deployed over *z*=1.5–55m on a 60m observational tower. At the time of the event occurrence, the atmospheric boundary layer was highly stable and the height of the LLJ was approximately 200m. Comparing this height to the LLJ height of δ =0.16m in the present wind tunnel experiment, we estimate the scale ratio to be 1/1250. In the wind tunnel experiment, turbulence bursting occurred at z=20-30mm. This height corresponds to *z*=25-38m in the atmosphere, based on the scale ratio above.

Nakamura and Mahrt (2005) also reported intermittent turbulence with CASES-99 tower measurements. Turbulence bursting frequently occurred at *z*=5m and turbulence bursting observed at this height is limited to a very thin layer. Their study found no general decrease of the gradient Richardson number prior to onsets of intermittent turbulence events.

As generation mechanisms of intermittent turbulence observed in atmospheric boundary layers, meso-scale disturbance, internal gravity waves and density currents are discussed in the literature. With no such external causes of intermittent turbulence, the present wind tunnel experiment may suggest a generation mechanism of intermittent turbulence which may be difficult to isolate in atmospheric boundary layers.

4. CONCLUSIONS

We simulated atmospheric stable boundary layers (SBL) with a low-level jet (LLJ) using a thermally stratified wind tunnel. We investigated the influence of the atmospheric stability on turbulence characteristics in SBLs with a strong shear near the surface.

Intermittent bursting of turbulence was generated in the lower portion of the SBL with high stability. This bursting originated aloft away from the surface and transported fluid with relatively low velocity and temperature upward and fluid with relatively high velocity and temperature downward.

Furthermore, we investigated the relationship between the occurrence of turbulence bursting and the local gradient Richardson number. The Ri number became larger than the critical Ri number, Ri_{cr} =0.25 in quiescent periods. On the other hand, the Ri number became smaller than Ri_{cr} during bursting events.

Acknowledgement

We would like to thank our students, H. Kokubu and K. Iwasaka of the Graduate School of Kyushu University and our laboratory staff, Messrs. K. Sugitani and K. Watanabe of Research Institute for Applied Mechanics, Kyushu University, for their assistance with the experiment and data analyses.

References

Kondo, J., Kanechika, O. and Yasuda, N. : Heat and Momentum Transfers under Strong Stability in the Atmospheric Surface Layer, J.

Atmos. Sci. 35 (1978) 1012-1021.

Mahrt, L. : Stratified Atmospheric Boundary Layers, Boundary-Layer Meteorol., 90 (1999) 375-396.

Nakamura, R., and Mahrt, L. : A study of intermittent turbulence with CASES-99 tower measurements, Boundary-Layer Meteorol., 114 (2005) 367-387.

Ohya, Y., Neff, D. E. and Meroney, R. N.: Turbulence structure in a stratified boundary layer under stable conditions', Boundary-Layer Meteorol., 83 (1997) 139-161.

Ohya, Y. : Wind tunnel study of atmospheric stable boundary layers over a rough surface, Boundary-Layer Meteorol., 98 (2001) 57-82.

Ohya, Y. and Uchida, T.: Turbulence Structure of Stable Boundary Layers with a Near-Linear Temperature Profile, Boundary-Layer Meteorol., 108 (2003) 19-38.

Ohya, Y., Tatsuno, M., Nakamura, Y., and Ueda, H. : A thermally stratified wind tunnel for environmental flow studies, Atmos. Environ., 30 (1996) 2881-2887.

Ohya, Y. and Fukamachi, N.: Development of a calibrator for thermo-anemometer, in Proc. 3rd Intl. Conf. on Fluid Dynamic Measurement and Its Applications, Beijing, China,(1997) 223-226.

Stull, R. B. : An Introduction to Boundary Layer Meteorology, Kluwer Academic Publishers, (1988) 499-502 and 513 (666).

Sun, J., Burns, S. P. and Lenschow, D. H. : Turbulence intermittency in the stable boundary layer, Proc. of the 14th Boundary Layer & Turbulence, Aspen, (2000) 329-331.

Sun, J, Burns, S, P. Lenschow, D. H., et al.: Intermittent turbulence associated with a density current passage in the stable boundary layer, Boundary-Layer Meteorol., 105 (2002) 199-219.

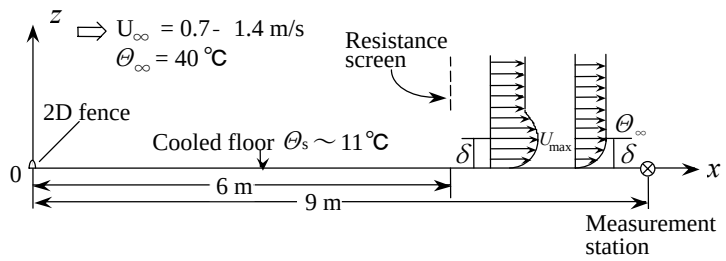

Fig.1. Experimental arrangement for SBL with low-level jet

	S1	S2
U_{max}(m/s)	1.51	1.18
Re_δ	16100	12600
Ri_δ	0.074	0.13
δ (m)	0.16	0.16
Θ_∞(℃)	39.3	39.2
Θ_S(℃)	11.4	10.8
$\Delta\Theta$(℃)	27.9	28.4
Θ_0(℃)	30.4	27.7
Symbol	○	□

Table1. Experimental data

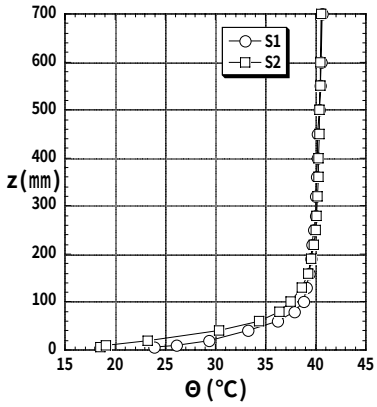

Fig.2. Vertical profiles of mean temperature Θ

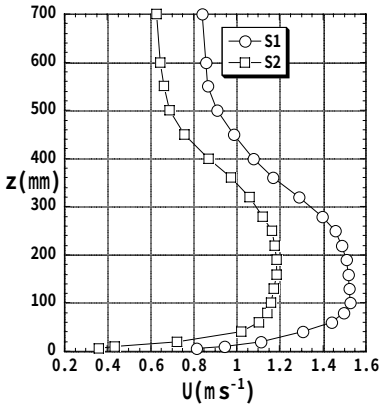

Fig.3. Vertical profiles of mean *U*-velocity

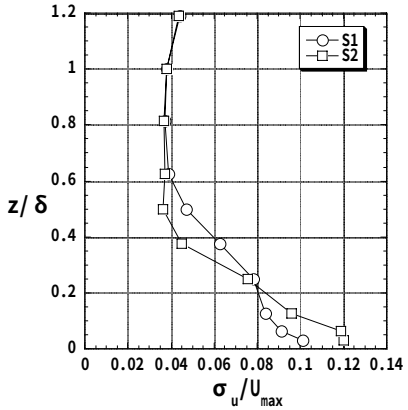

Fig.4. Vertical profiles of *u*-velocity fluctuation

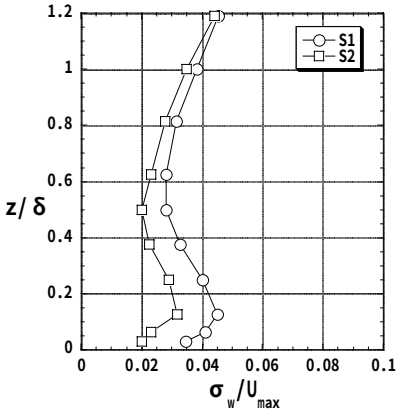

Fig.5. Vertical profiles of *w*-velocity fluctuation

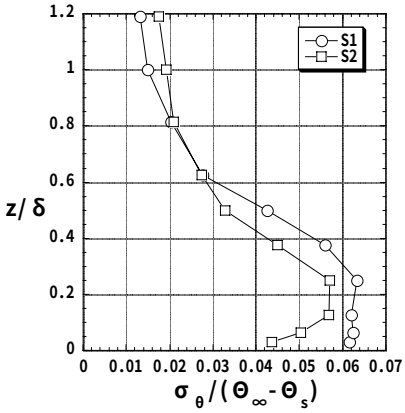

Fig.6. Vertical profiles of temperature fluctuation

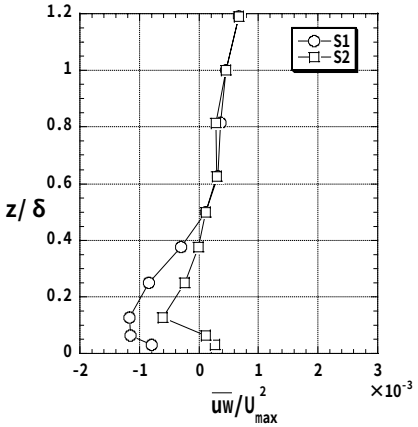

Fig.7. Vertical profiles of momentum flux $\overline{uw}$

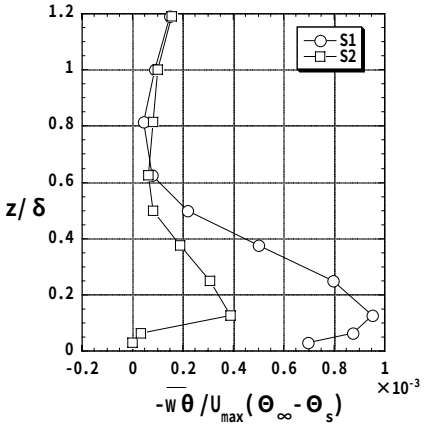

Fig.8. Vertical profiles of heat flux $\overline{w\theta}$

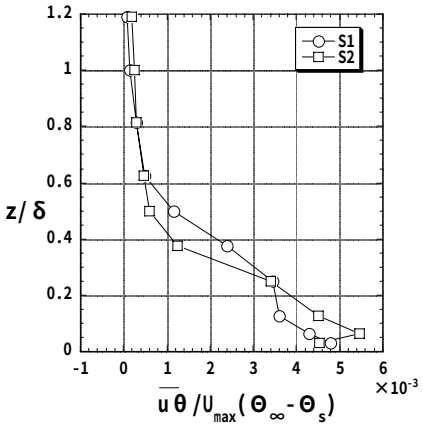

Fig.9. Vertical profiles of heat flux $\overline{u\theta}$

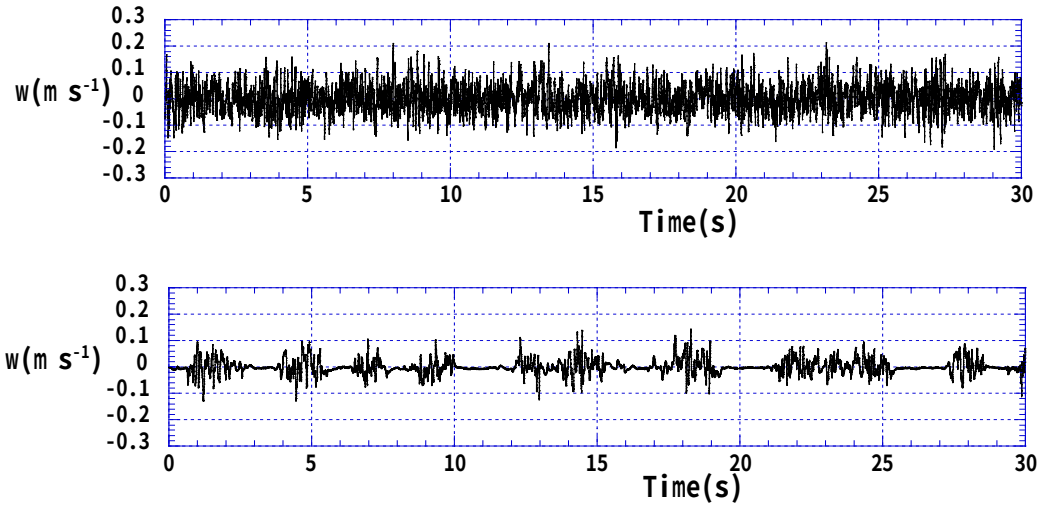

Fig.10. Time histories of w-velocity fluctuation at z=20mm (upper, Case S1; lower, Case S2)

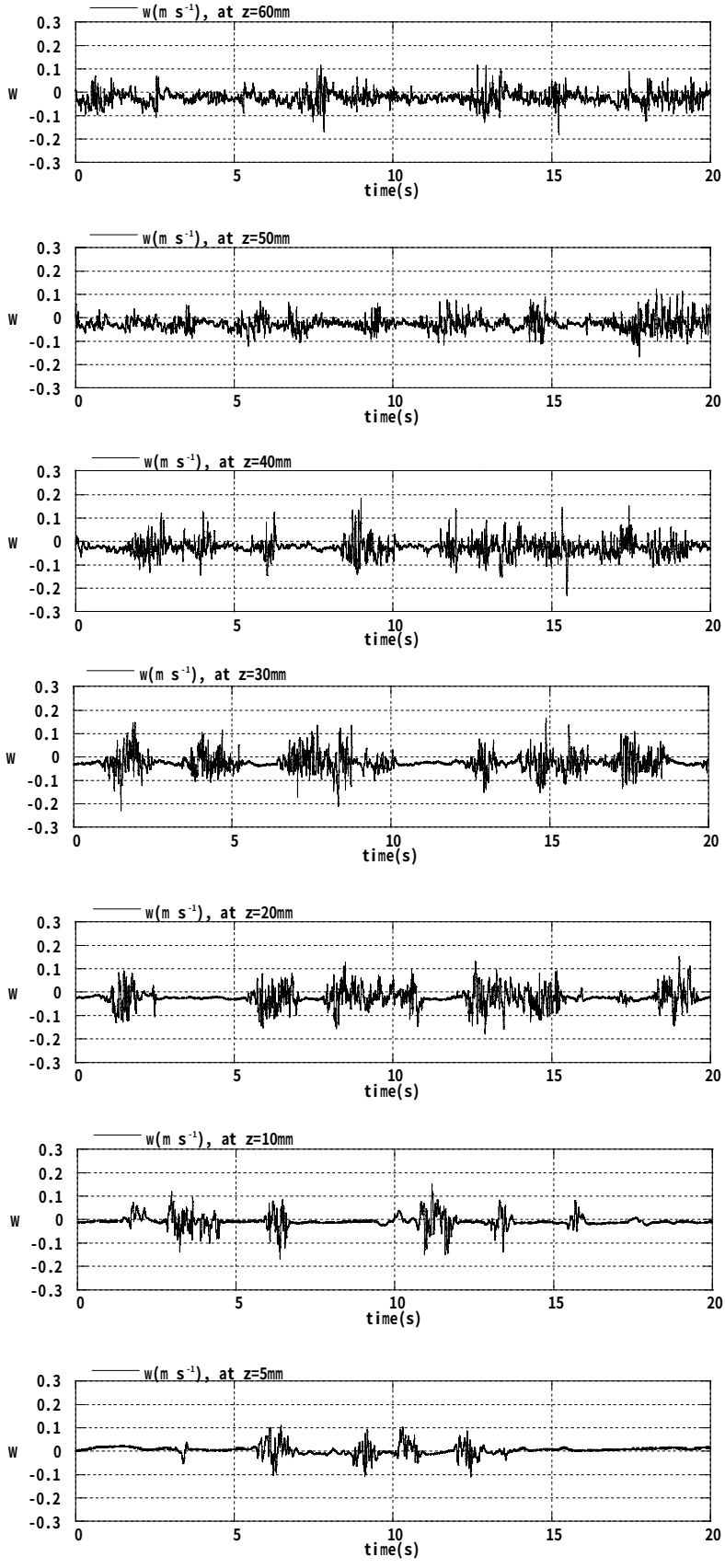

Fig.11. Time histories of *w*-velocity fluctuation at *z*=5-60 mm (Case S2)

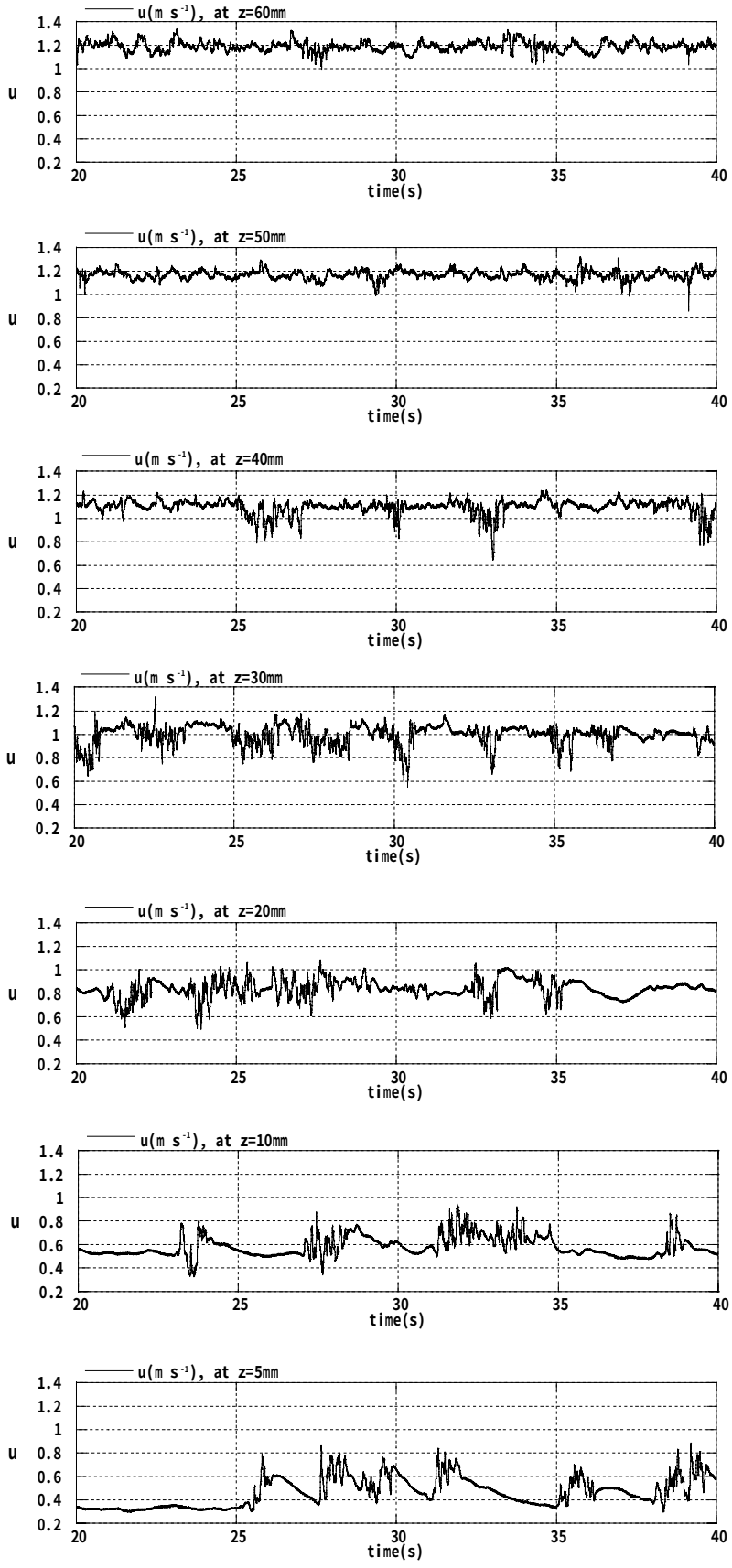

Fig.12. Time histories of *u*-velocity fluctuation at *z*=5-60mm (Case S2)

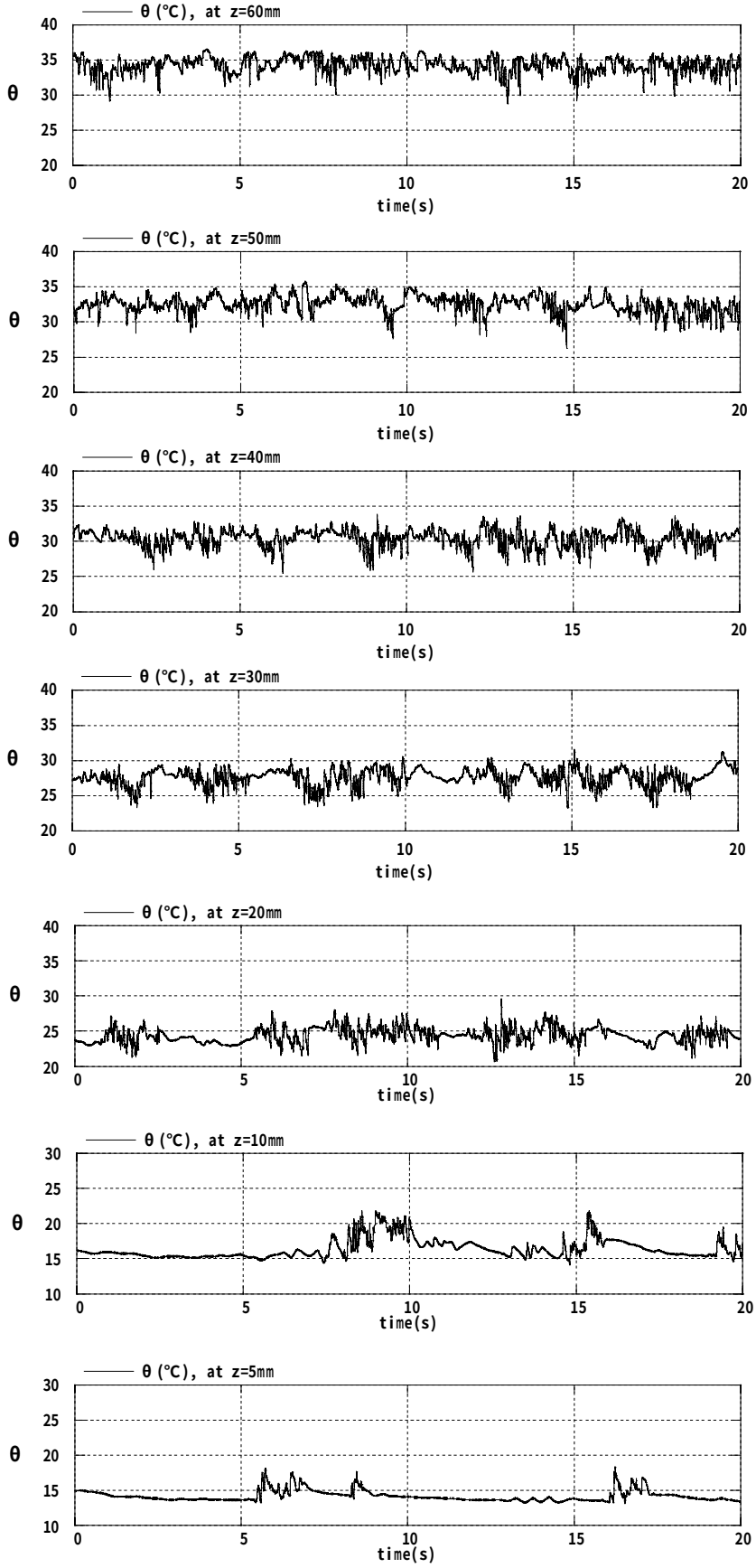

Fig.13. Time histories of temperature fluctuation at z=5-60 mm (Case S2)

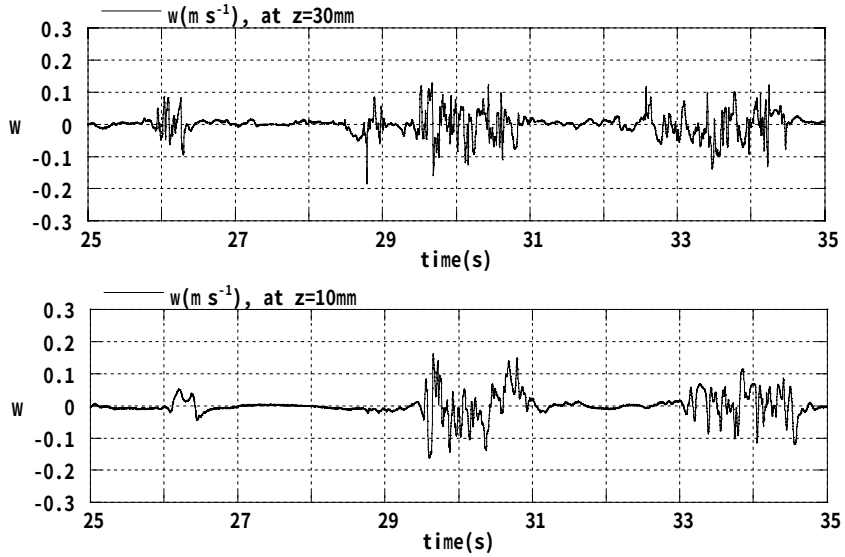

Fig.14. Simultaneous measurement of w-velocity fluctuations at two different heights (upper, z=30mm ; lower, z=10mm), Case S2.

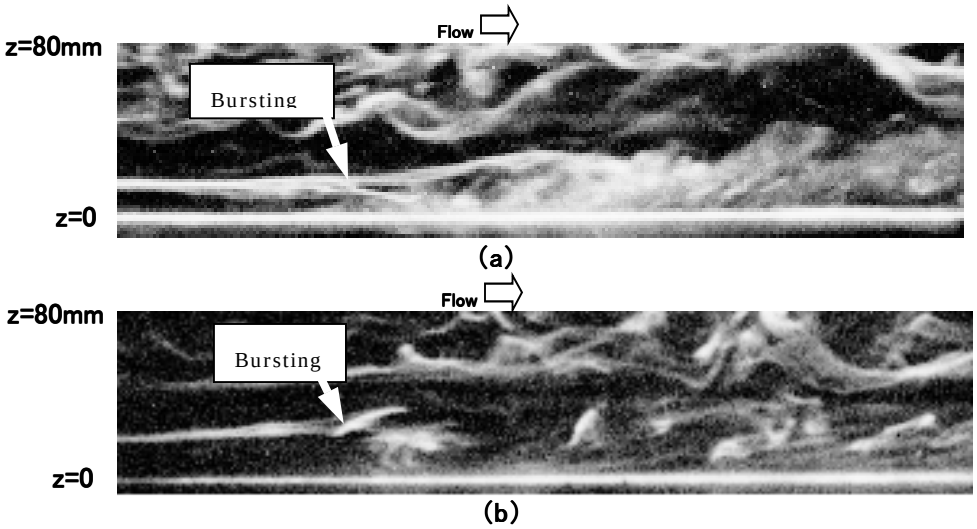

Fig.15. Flow visualization of SBL with low-level jet (Case S2). Side view of around x=9m. Flow is left to right. A turbulent bursting event occurs.

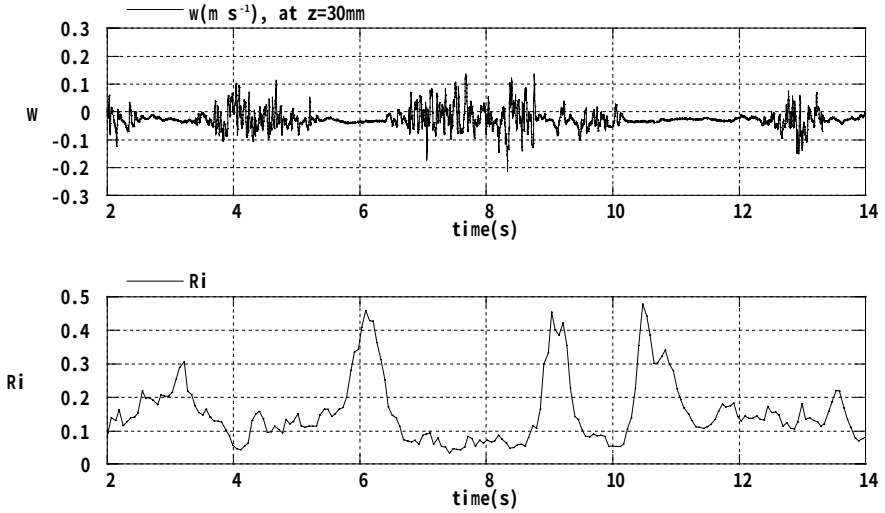

Fig.16. Time histories of w-velocity fluctuation and corresponding Richardson number at z=30mm, Case S2.